New Journal of Physics
The open–access journal for physics

Charge-transfer polaron induced negative differential resistance and giant magnetoresistance in organic spin-valve systems

J H Wei[1,2,4], S J Xie[1], L M Mei[1], J Berakdar[3] and YiJing Yan[2,4]

[1] Department of Physics, Shandong University, Jinan, People's Republic of China
[2] Department of Chemistry, Hong Kong University of Science and Technology, Kowloon, Hong Kong
[3] Max-Planck Institut für Mikrostrukturphysik, 06120 Halle, Germany
E-mail:wjh@sdu.edu.cn, yyan@ust.hk

New Journal of Physics **8** (2006) 82
Received 23 February 2006
Published 30 May 2006
Online at http://www.njp.org/
doi:10.1088/1367-2630/8/5/082

Abstract. Based on the static polaron Su–Schrieffer–Heeger model and the nonequilibrium Green's function formalism, we investigate the negative differential resistance (NDR) effect in organic spin-valve systems at low temperature and interpret it with a self-doping picture. A giant negative magnetoresistance exceeding 300% is theoretically predicted as the results of the NDR effects.

The discovery of negative differential resistance (NDR) in traditional semiconductor diodes [1] and also organic semiconductor (OSE) nanostructures [2, 3] has opened a new chapter of device physics. Motivated by the potential applications of organic NDR, numerous experiments have been done with different OSE electronic devices [4]–[7]. Although some possible mechanisms have been suggested, the organic NDR remains a theoretical challenge, beyond the simple picture of interband tunnelling or resonant tunnelling in the heterostructure. The organic NDR concerns not only the excess charge transfer through lead/OSE/lead structures [2], [8]–[10], but also the strong electron–phonon (e-ph) coupling [11] that induces polarons in OSE structures [12].

Historically, the discovery of a giant magnetoresistance (GMR) effect in 1988 is considered as the beginning of a new technology called spintronics [13]–[17], where it is not only electron charge but electron spin that carries information. In addition to inorganic semiconductors [18, 19], OSE materials, due to their controllable structure, strong e-ph coupling [11], and large spin

[4] Authors to whom any correspondence should be addressed.

PII: S1367-2630(06)19593-2

coherence [20], offer another promising system to spintronics [21, 22]. In a recent experiment of spin-injection in a spin-valve structure LSMO/Alq_3/Co, a GMR as large as 40% had been detected[5] [22]. In this paper, we report the possibility of a charge-transfer polaron-induced NDR mechanism via a numerical study on a representing π-conjugated OSE model device that exhibits also a GMR.

In the study of the electronic conductivity and optical phenomena in π-conjugated OSEs, the Su–Schrieffer–Heeger (SSH) model [23] has also shown a remarkable track of success. This model captures the essential characteristic of a conjugated molecule, where the strong e-ph coupling leads it to the polaron (or soliton) charged states and dimerized ground state. In addition to polyacetylenes, the SSH model has been applied to charged-conjugated systems [24] carbon nanotubes [25], and DNA molecules [26, 27]. In this work, the SSH Hamiltonian for the OSE electrons coupled adiabatically with lattice displacements reads

$$H_{\mathrm{O}} = \sum_{n,\sigma} \{\epsilon_o c^+_{n,\sigma} c_{n,\sigma} - [t_o - (-1)^n t_1 - \alpha_o y_n](c^+_{n,\sigma} c_{n+1,\sigma} + \mathrm{H.c.})\} + \frac{K_o}{2} \sum_n y_n^2. \tag{1}$$

Each atomic unit in OSE is represented by a single normalized site; $c^+_{n,\sigma}$ ($c_{n,\sigma}$) denotes the creation (annihilation) operator of an electron at the nth site with spin σ, while ϵ_o, t_o and t_1 are the on-site energy, zero-displacement hopping integral, and nondegeneracy parameter, respectively. The lattice distortion is treated classically in terms of the bond distances $\{y_n = u_{n+1} - u_n\}$, deviated from its energy-minimum values that are to be determined via the Hellmann–Feynman theorem (cf equation (7)), with the spring constant K_o and the adiabatic e-ph coupling constant α_o. This is a static polaron model which, together with the effective noninteracting many-electron ansatz in equation (1), is considered to be justifiable in the present study of stationary transport (Born–Oppenheimer approximation). On the other hand, the question of polaron dynamics in comparison to the external parameter change will become a crucial issue in describing the dependence of current–voltage characteristic on bias voltage sweep rate and sweep direction. We will consider this problem in future work.

Further, we choose a symmetric ferromagnetic (FM) 3d transition metal as electrodes. The spin-dependent charge transport takes place between their 3d bands. Neglecting spin flip during transport and adopting the two-current model [28], we describe the FM metal by one-dimensional single d-band tight-binding model with a spin splitting term [11],

$$H_{\mathrm{F}} = \sum_{n,\sigma} \left[\epsilon_f d^+_{n,\sigma} d_{n,\sigma} + t_f (d^+_{n,\sigma} d_{n+1,\sigma} + \mathrm{H.c.})\right] - \sum_n J_f (d^+_{n,\uparrow} d_{n,\uparrow} - d^+_{n,\downarrow} d_{n,\downarrow}), \tag{2}$$

where $d^+_{n,\sigma}$ ($d_{n,\sigma}$) is the creation (annihilation) operator of an electron in the metal at the nth site with spin σ; ϵ_f is the on-site energy of a metal atom, t_f is the nearest-neighbour transfer integral, and J_f is the Stoner-like exchange integral. The coupling between the OSE and FM electrodes is described by the spin-independent hopping integral, $t_{c\mathrm{L}} = t_{c\mathrm{R}} = \beta(t_f + t_o)$, where β denotes the OSE-metal binding parameter.

The nonequilibrium Green's function approach based on the Keldysh formalism [29]–[31] is used to calculate the quantum transport properties of organic spintronics. To do that, the spintronic device is divided into three distinct regions. One is the so-called central scattering region (S-region), with the Hamiltonian $H_{\mathrm{S}} = H_{\mathrm{L}} + H_{\mathrm{O}} + H_{\mathrm{R}} + H_{\mathrm{int}}$, which consists of the OSE together with a small number of metal atoms attached to each of its ends. The other two are

[5] LSMO is $La_{0.7}S_{0.3}MnO_3$.

electrodes (L and R) that serve as charge reservoirs with the steady-state electronic distribution of bulk metal at a given temperature. Tracing out the reservoir degrees of freedom leads to an effective S-region retarded Green's function

$$G(E) = [ES - H_S - \Sigma_L(E) - \Sigma_R(E)]^{-1}. \tag{3}$$

Here, S (set to be the unit matrix) is the overlap integral matrix between basis wave functions, while $\Sigma_{L/R}$ is the self-energy matrix that accounts for the effects of reservoir electrodes on the S-region [30]. It is possible to have the analytical solution of $\Sigma_{L/R}$ for the one-dimensional FM metal transfer-coupling with the OSE system. In this work, we adopt an efficient numerical approach through solving eigenvalue equations to achieve the self-energy [32]. This approach can be easily extended to study the magneto-transport beyond the one-dimensional system.

The current can be evaluated in the mean-field or effective one-electron picture as [30]

$$I = \frac{e}{h}\int_{-\infty}^{\infty} \mathrm{Tr}(\Gamma_L G \Gamma_R G^{\dagger})[f(E,\mu_L) - f(E,\mu_R)]\,\mathrm{d}E. \tag{4}$$

$\Gamma_{L/R} \equiv \mathrm{i}(\Sigma_{L/R} - \Sigma_{L/R}^{\dagger})$ denotes the broadening matrix, while $f(E,\mu_{L/R})$ is the Fermi distribution function at the lead chemical potential $\mu_{L/R}$. The trace term in the integrand, where the trace (Tr) runs over the electronic spin–orbital space, is the transmission coefficient function. As the effect of spin flip on transport is not considered in this work, equation (4) consists of the spin-up and spin-down contributions. This fact is rooted in the model, where H_O for OSE, H_F for FM and H_{int} for the interaction between them are all spin block diagonal (cf equations (1) and (2)), and so for the resulting Green's functions and related matrices.

One can also evaluate the density of states (DOS) via $D(E) = \mathrm{i}\mathrm{Tr}[G(E) - G^{\dagger}(E)]/(2\pi)$, and the reduced density matrix via

$$\rho = \frac{1}{2\pi}\sum_{\alpha=L,R}\int_{-\infty}^{\infty} G\Gamma_\alpha G^{\dagger} f(E,\mu_\alpha)\,\mathrm{d}E, \tag{5}$$

with a given number of carrier electrons $N = \mathrm{Tr}\,\rho$ in the S-region. We separate the reduced density matrix into its equilibrium and bias-induced contributions, and evaluate them by contour integration and direct multi-grid Gaussian integration, respectively. Numerical implementation will be carried out in a real-function basis set representation, and the resulting ρ will be real [31].

We take the bias V not changing the electronic structures of L and R reservoirs, but just shifting their potentials by $V/2$ and $-V/2$, respectively. In contrast, it does alter the Hamiltonian of OSE to become $H_O - e\phi(x)$. The electric potential drop here, satisfying $\phi(x_1) = V/2$ and $\phi(x_{N_o}) = -V/2$, should be evaluated via Poisson's equation with the method of images [33]

$$\nabla^2\phi(x) = -\sum_{n=1}^{N_o}\frac{\rho_{nn}}{\varepsilon_0}\delta(x_n - x). \tag{6}$$

Here, ε_0 is the vacuum permittivity, $\rho_{nm} = \sum_\sigma \rho_{nm}^{\sigma}$, and $x_n = u_n + (n-1)a$ with a being the OSE lattice constant at equilibrium. The on-site charge density ρ_{nn} in equation (6) depends not only on $\phi(x)$, but also on the lattice distortion parameter u_n due to the e-ph interaction. In general, the dependence of electron wavefunction (or ρ_{nm}) on the lattice distortion parameters can be obtained

via the variation principle. The Hellmann–Feynman theorem, i.e., $\partial[\mathrm{Tr}(H_S\rho)]/\partial y_n = 0$, leads to (cf equation (1) with $y_n \equiv u_{n+1} - u_n$)

$$2\alpha_o(\rho_{n,n-1} - \rho_{n+1,n}) + K_o(y_{n-1} - y_n) = 0. \tag{7}$$

The index n here includes only the OSE sites, since there are no lattice distortions in the L and R sub-structures. The Hellmann–Feynman theorem was originally formulated for the ground (equilibrium) state situation. Recently, Ventra and Pantelides have shown that it also applicable for the steady-state transport problem, at least for its DFT-based formalism [34]. From equations (5)–(7), one can see that both the charging effect from the electrodes and the external potential from the bias voltage are all included in the nonequilibrium density matrix of the coupled e-ph system which should be evaluated self-consistently.

There are two distinct transport measurement configurations, parallel (P) and antiparallel (AP), with respect to the relative magnetization orientation of two FM electrodes. Generally, in the two-current model, both the majority–majority and minority–minority (or majority–minority and minority–majority) transports are permitted in the P (or AP) configuration. But for the cobalt electrodes in the present work, the full-filled up-spin electrons cannot transport in the P-configuration and the charge carriers are only the half-filled down-spin electrons. In contrast, the charge carriers in the AP-configuration under $V > 0$ are only the up-spin electrons, driven from the full-filled majority-spin band of L-electrode to the half-filled minority-spin band of R-electrode of opposite magnetization orientation.

We are now in a position to elucidate numerically the I–V characteristics, especially the NDR behaviour of OSE systems. The SSH parameters for the OSE system (equation (1)) are $\epsilon_o = -4.3$ eV, $t_o = 2.5$ eV, $t_1 = 0.04$ eV, $\alpha_o = 5.0$ eV Å^{-1}, and $K_o = 21.0$ eV Å^{-2}, which are the modified values from those of conducting polymers [35] for the OSE being of larger band gap. The tight-binding parameters for the cobalt electrodes (equation (2)) are $\epsilon_f = -7.0$ eV, $t_f = 1.5$ eV and $J_f = 1.45$ eV, determined by fitting the cobalt 3d band structure [36]. The OSE-metal binding parameter β will be specified later.

To justify the above values, we calculated the band structures of the model OSE and FM cobalt electrodes individually (with $\beta = 0$); see figure 1(a) for their resulting DOS at $T = 11$ K. Our model OSE of ten sites has the highest occupied and lowest unoccupied molecular orbitals of $E_{\mathrm{HOMO}} = E_F - 0.9$ eV and $E_{\mathrm{LUMO}} = E_{\mathrm{F}} + 2.0$ eV, where E_{F} is the Fermi level of the cobalt electrode. These results well reproduce the band gap diagram of the OSE spin-valve device used in a recent experiment [22]. The model cobalt metal is also consistent with the real material [36], which shows one full-filled majority-spin band, and one half-filled minority-spin band.

Let us start with the equilibrium property of the model spintronic system at $V = 0$, at which the S-region (Co/OSE/Co) assumes charge neutral. In our model, the S-region consists of a cobalt oligomer of 10-sites to each terminal of the ten-site OSE; thus each segment in Co/OSE/Co involves 20 spin-orbitals. If the OSE-metal binding parameter $\beta = 0$, three segments of the S-region would be charge neutral individually, with $N_{\mathrm{L}} = N_{\mathrm{R}} = 15$ and $N_O = 10$ electrons, respectively. In reality, $\beta \neq 0$ and intra-regional charge transfer (ICT) is possible. Depicted in figure 1(b) is the calculated DOS of the organic spintronic device with the OSE-metal binding parameter $\beta = 0.5$, where an ICT of about $1.14e$ from OSE to Co-segments has occurred. The observed 'self-doping' phenomenon here is largely due to the strong e-ph interaction, which leads to the formation of a pre-existing hole polaron that stabilizes the S-region complex before applying potential bias [37]. The pre-existing hole polaron state is rather evident by examining

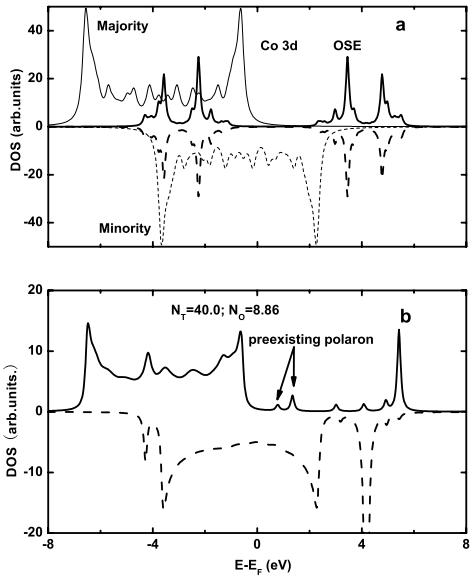

Figure 1. DOS of the majority-spin (solid curves) and minority-spin (dash curves) bands of model systems: (a) the isolated OSE (thick curves) and Co 3d band (thin curves), with the OSE-metal binding parameter $\beta = 0$; (b) the binded Co/OSE/Co spintronic device with $\beta = 0.5$. Temperature $T = 11$ K.

the majority-spin band of Co/OSE/Co complex (solid curve in figure 1(b)), since its isolated metal counterpart (thick-solid curve in figure 1(a)) is completely filled up to the Fermi level.

We then calculated the I–V characteristic (equation (4)) of the model Co/OSE/Co spintronics at $T = 11$ K and $\beta = 0.5$, in both the P and AP configurations of relative magnetization orientation of FM electrodes. The resulting I–V curves in these two configurations (P: solid; AP: dash) are shown in figure 2(a), and the corresponding $\mathrm{d}I/\mathrm{d}V$ ones are in figure 2(b). Included in figure 2(b) is also a thick curve for the bias voltage dependence of magnetoresistance (MR), $\Delta R/R = (R_{\mathrm{AP}} - R_{\mathrm{P}})/R_{\mathrm{AP}}$, measuring the relative difference of electric resistance with these two configurations.

Consider first the NDR behaviour (about $-26.3\,\mathrm{k}\Omega$ at its minimum) in the P-configuration, where the current, after an initial near-ohmic increase, drops quickly from $I_{\mathrm{peak}} = 4.45$ μA at $V_{\mathrm{peak}} = 0.35$ V to $I_{\mathrm{valley}} = 0.49$ μA at $V_{\mathrm{valley}} = 0.4$ V. To see what happens during the NDR region, we also examined other nonequilibrium properties (at $V > 0$). Shown in figure 3 are the representing results of both the current peak (solid) and valley (dash) states: (i) the majority-spin (up-spin) DOS $D(E)$ and (ii) the P-configuration (down-spin) transmission coefficient function $T(E)$. Indicated in figure 3 are also the numbers of electrons in the OSE segment at the two corresponding voltages. By checking the charge distribution and the lattice distortion (not shown here), we found: (i) the preexisting hole polaron remains localized around the OSE centre when $0 \leqslant V \leqslant V_{\mathrm{peak}}$; (ii) as V increases further, the excess electron charge migrates from the leads into the OSE segment; and (iii) at $V_{\mathrm{valley}} = 0.4$ V, the preexisting hole is completely annihilated, and the OSE is essentially in its dimerized ground charge-neutral state.

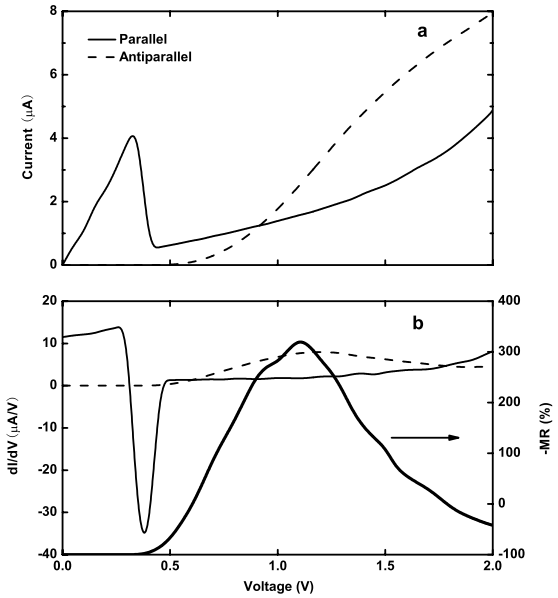

Figure 2. (a) The I–V characteristics of the Co/OSE/Co system in figure 1(b), measured with the P- (solid curve) and AP-configuration (dash curve) of relative magnetic orientation of electrodes. (b) The $\mathrm{d}I/\mathrm{d}V$, obtained numerically via (a), and $-\Delta R/R$ (thick line) as functions of the bias voltage.

The above observations suggest that the NDR behaviour in the P-configuration, shown by the solid curves in figure 2, is due to the annihilation of the pre-existing, 'self-doping' hole polaron. As discussed earlier (cf figure 1(b)), the pre-existing hole polaron level at $V = 0$ deeply localizes in the down-spin band (P-configuration conduction band) gap of the OSE, which leads to its relatively large DOS, and thus a low-resistance state according to the doping theory of conducting polymers [35]. This accounts for the rapid increase of current when $V < V_{\mathrm{peak}}$ in the P-configuration (the solid curve in figure 2(a)).

Figure 3 shows clearly that the increase of bias voltage from V_{peak} to V_{valley} accompanies the annihilation of the pre-existing polaron, which accounts for the NDR observed in the P-configuration (solid curves) in figure 2.

In the AP configuration, the charge carriers at $V > 0$ are no longer the down-spin electrons, but the up-spin ones, from the majority subband of L to the minority subband of R electrode. As the observed switch-on voltage in this case (about 0.5 V) exceeds the aforementioned NDR region, the 'pre-existing polaron' makes no direct contribution to the conductance in the AP configuration. The resulting I–V characteristic (dash curve in figure 2(a)) can thus be understood (including its switch-on voltage) by examining the structures of the two involving subbands in figure 1(b) at $V = 0$.

Finally, let us comment on the voltage-dependent MR (the thick curve in figure 2(b)), especially the negative GMR of $(-\Delta R/R)_{\mathrm{max}} = 300\%$ at $V = 1.1$ V. Negative MR has been experimentally observed in the $\mathrm{Co/SrTiO_3/LSMO}$ tunnel junction [38] and the LSMO/OSE/Co spin-valve device [22]. Traditionally, one analyses the observed MR, or other transport behaviour as function of bias potential, via the involving DOS of conduction bands/subbands of uncorrelated ($\beta = 0$) FM/OSE/FM systems at $V = 0$, such as figure 1(a) and [36]. This

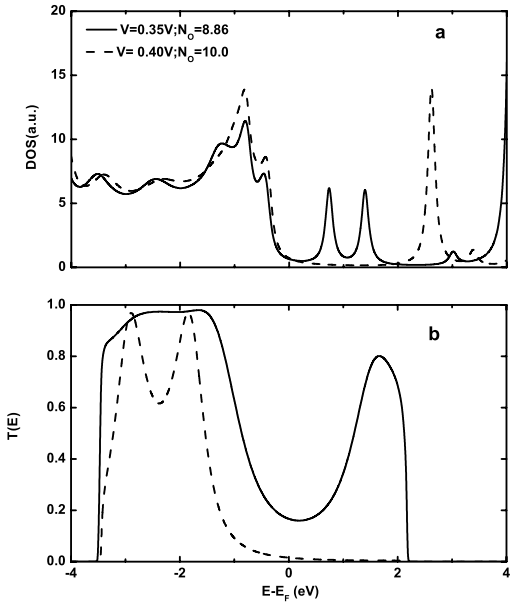

Figure 3. The current-peak state (solid lines) and the valley state (dash lines), referring to the I–V characteristic of the parallel configuration in figure 2(a), in terms of (a) the DOS of majority-spin band and (b) the transmission coefficient of electrons (minority-spin). The total numbers of electrons in the OSE segment in the current-peak and valley states are specified.

traditional analysis does lead to our understanding the qualitative MR–V behaviour in each individual voltage range in figure 2(b), where $\Delta R/R$ decreases from 100%, changes sign into the negative MR region, reaches $(-\Delta R/R)_{\max}$ at $V = 1.1$ V, and etc. However, the quantitative GMR values in figure 2(b), especially its maximum value of 300%, cannot be accounted for via the simple band structure analysis with $\beta = 0$ and/or $V = 0$. The calculated extraordinary GMR of 300% can only be accounted for via the 'self-doping' of the pre-existing polaron and its annihilation that distinctly differently affect conductances depending on the (P or AP) relative magnetization orientation of FM electrodes.

In summary, we proposed to exploit 'self-doping' $FM_1/OSE/FM_2$ structures for distinct NDR and GMR materials. Numerical demonstrations were performed based on a model Hamiltonian with realistic parameters for the system. The theoretical NDR was found as a result of transition from the low-resistant pre-existing hole (cation) polaron to high-resistant dimerized charge-neutral ground state. This NDR mechanism is different from the two-step reduction picture, proposed originally by Reed and co-workers [2] in explaining their experiment on a redox-centre-containing molecule, in which NDR results in transition from conducting anion to insulating dianion state. As it appears in the P- but not AP-configuration of relative magnetization orientation of FM electrodes, the NDR leads also to a large magnitude (300%) of negative GMR, much larger than the experimentally reported ones so far [22]. Many OSEs are easy-doping materials [35], and the required 'pre-existing polaron' state can be formed in either self-doping or external doping manner. Thus, experimental realizations of GMR far exceeding 100% in organic spintronic devices should be feasible according to the present model study.

The charge-transfer polaron-induced NDR effect studied in this work may also shed some light on a recent experiment [39]. The observed hysteretic NDR behaviour there has been interpreted in terms of charge capture and release processes, which in a sense are equivalent to the formation and annihilation of the charge-transfer polaron state in this work. Our present study is however based on the steady-state polaron transport theory, involving the static polaron approximation, together with the effective single-electron picture and the quasi-equilibrium Hellmann–Feynman theorem. To study the observed dependence of NDR on the sweep direction and sweep rate of applied bias [39], one should go beyond the present theory, to include at least the kinetics of polaron states in the timescale of external parameter change.

Acknowledgments

Support from the Research Grants Council of the Hong Kong Government (604804) and the National Natural Science Foundation of China (Grant no 10474056) are gratefully acknowledged.

References

[1] Sze S M 1990 *High-Speed Semiconductor Devices* (New York: Wiley)
[2] Reed M A, Rawlett A M and Tour J M 1999 *Science* **286** 1550
[3] Chen J, Wang W, Reed M A, Rawlett A M, Price D W and Tour J M 2000 *Appl. Phys. Lett.* **77** 1224
[4] Kratochvilova I, Kocirik M, Zambova A, Mbindyo J, Mallouk c T E and Mayerc T S 2002 *J. Mater. Chem.* **12** 2927
[5] Walzer K, Marx E, Greenham N C, Less R J, Raithby P R and Stokbro K 2004 *J. Am. Chem. Soc.* **126** 1229
[6] Rawlett A M, Hopson T J, Amlani I, Zhang R, Tresek J, Nagahara L A, Tsui R K and Goronkin H 2003 *Nanotechnology* **14** 377
[7] Rawlett A M, Hopson T J, Amlani I, Zhang R, Tresek J, Nagahara L A, Tsui R K and Goronkin H 2005 *Nano Lett.* **4** 55
[8] Xue Y, Datta S, Hong S, Reifenberger R, Henderson J I and Kubiak C P 1999 *Phys. Rev.* B **59** R7852
[9] Karzazi Y, Cornil J and Brédas J L 2003 *Nanotechnology* **14** 165
[10] Emberly E G and Kirczenow G 2001 *Phys. Rev.* B **64** 125318
[11] Xie S J, Ahn K H, Smith D L, Bishop A R and Saxena A 2003 *Phys. Rev.* B **67** 125202
[12] Galperin M, Ratner M A and Nitzan A 2005 *Nano Lett.* **5** 125
[13] Baibich M N, Broto J M, Fert A, Dau F N V, Petroff F, Eitenne P, Creuzet G, Friederich A and Chazelas J 1988 *Phys. Rev. Lett.* **61** 2472
[14] Barnas J, Fuss A, Camley R E, Grünberg P and Zinn W 1990 *Phys. Rev.* B **42** 8110
[15] Moodera J S, Kinder L R, Wong T M and Meservey R 1995 *Phys. Rev. Lett.* **74** 3273
[16] Wolf S A, Awschalom D D, Buhrman R A, Daughton J M, von Motnár S, Roukes M L, Chtchelkanova A Y and Treger D M 2001 *Science* **294** 1488
[17] Žutić I, Fabian J and Sarma S D 2004 *Rev. Mod. Phys.* **76** 323
[18] Kikkawa J M and Awschalom D D 1999 *Nature* **397** 139
[19] Yan S S, Ren C, Wang X, Xin Y, Zhou Z X, Mei L M, Ren M J, Chen Y X, Liu Y H and Garmestani H 2004 *Appl. Phys. Lett.* **84** 2376
[20] Krinichnyi V I 2000 *Synth. Met.* **108** 173
[21] Dediu V, Murgia M, Matacotta F C, Taliani C and Barbanera S 2002 *Solid State Commun.* **122** 181C184
[22] Xiong Z H, Wu D, Vardeny Z V and Shi J 2004 *Nature* **427** 821
[23] Su W P, Schrieffer J R and Heeger A J 1980 *Phys. Rev.* B **22** 2099
[24] Torii H J 2000 *J. Phys. Chem.* A **104** 413

[25] Wei J H, Xie S J, Wang S G and Mei M L 2001 *Phys. Lett.* A **292** 207
[26] Conwell E M and Rakhmanova S V 2000 *Proc. Natl Acad. Sci. USA* **97** 4556
[27] Wei J H, Wang L X, Chan K S and Yan Y 2005 *Phys. Rev.* B **72** 064304
[28] Fert A 1969 *J. Phys. C Solid State Phys.* **2** 1784
[29] Keldysh L V 1965 *Sov. Phys.—JETP* **20** 1018
[30] Datta S 1995 *Electronic Transport in Mesoscopic Systems* (New York: Oxford University Press) 1995
[31] Brandbyge M, Mozos J L, Ordejón P, Taylor J and Stokbro K 2002 *Phys. Rev.* B **65** 165401
[32] Ando T 1991 *Phys. Rev.* B **44** 8017
[33] Jackson J D 1975 *Classical Electrodynamics* (New York: Wiley)
[34] Ventra M D and Pantelides S T 2000 *Phys. Rev.* B **61** 16207
[35] Heeger A J, Kivelson S, Schrieffer J R and Su W P 1988 *Rev. Mod. Phys.* **60** 781
[36] Papaconstantopoulos D A 1986 *Handbook of the Band Structure of Elemental Solids* (New York: Plenum)
[37] Brédas J L and Street G B 1985 *Acc. Chem. Res.* **18** 309
[38] De Teresa J M, Barthélémy A, Fert A, Contour J P, Lyonnet R, Montaigne F, Seneor P and Vaurès A 1999 *Phys. Rev. Lett.* **82** 4288
[39] Kiehl R A, Le J D, Candra P, Hoye R C and Hoye T R 2006 *Appl. Phys. Lett.* **88** 172102